

Influence of Temperature on the Corrosion Behavior of X80 Steel in an Acidic Soil Environment

Yuanhui Wu^{1,2,*}, Suxing Luo^{1,2}, Qingsong Mou^{1,2}

¹ Department of Chemistry and Chemical Engineering, Zunyi Normal College, Zunyi, 563006, P. R. China.

² Special Key Laboratory of Electrochemistry for Materials of Guizhou Province, Zunyi, 563006, P. R. China

*E-mail: yhwull@126.com

Received: 8 September 2019 / Accepted: 26 October 2019 / Published: 30 November 2019

The influence of temperature on the corrosion behavior of X80 steel in an acidic soil environment was determined using electrochemical and surface analysis methods. The results revealed that the corrosion rate of X80 steel increased with increasing soil temperature from 25 °C to 75 °C, and the corrosion rate of X80 steel at 75 °C was 19 times higher than that at 25 °C. The charge transfer resistance decreased with increasing soil temperature, and the control step for corrosion was the activation polarization process. The kinetics of the corrosion process complied with the Arrhenius law, and the activation energy E_a was 50.7 kJ·mol⁻¹. In addition, the compositions of corrosion products consisted of Fe₂O₃, Fe₃O₄, SiO₂ and Al₂O₃.

Keywords: X80 steel; soil; corrosion; temperature

1. INTRODUCTION

Soil as a corrosive medium generally has a greater complexity than other environments [1]. Compared with general corrosion media, a soil medium has many distinct characteristics, such as diversity, immobility, nonuniformity, seasonality and regionality. Many factors affect soil corrosiveness, including soil type, soil temperature, moisture content, resistivity, pH, dissolved ions and oxygen, redox potential, chemical species and quantity of microorganisms in soil [2-9]. The change in soil temperature due to changing seasons and the temperature variance due to oil and gas being transported in a pipeline affect the corrosion of metals in the soil. As a result, temperature is an important factor in the evaluation of soil corrosivity, which can modify the interactions between the metal and the soil conditions.

The corrosion of underground structures has resulted in a high degree of environmental, human and economic consequences all around the world [10]. Therefore, it is urgent to study the corrosion

behavior of buried metallic structures. However, in the past few years, little research has been conducted on the influence of temperature on the corrosion of buried metallic structures. Most studies related to the temperature influence on buried metallic structures are focused on the inside temperature of the structure but not the outside temperature of the surrounding soil. Some researchers have investigated the temperature dependence of metal corrosion in aqueous solutions [11-13], but not in real soil. X80 steel has the advantages of a low cost and high strength and toughness along with having broad application potential in gas pipeline construction [14, 15].

The soil samples used in the study represent a typical acidic soil. Literature surveys reveal that owing to some unique properties of the acidic soil, including low pH value, high soil resistivity and high soil moisture, the acidic soil is highly corrosive, which is different from alkaline and neutral soils [16, 17].

In this study, the influence of temperature on the corrosion behavior of X80 steel in an acidic soil environment was investigated. The purpose of this study is to provide insight into the outside temperature influence on the corrosion of buried metallic structures.

2. EXPERIMENTAL

2.1 Materials

Working electrodes were made with X80 steel with the following composition (wt%): C-0.043, Si-0.190, Mn-1.692, P-0.010, S-0.003, Mo-0.102, Ni-0.229, Cr-0.027, Cu-0.141, and Fe-balance. X80 steel was embedded in an epoxy resin, leaving a surface area of 1 cm². The specimens were polished with emery papers from 400-1000 grade and then cleaned with ethanol. The electrodes were dried and kept in a desiccator.

2.2 Soil samples

Soil samples were taken from Zunyi (27°42' N, 106°55' E), China. The soil type was a typical acidic and yellow soil. Table 1 shows the compositions and pH values of the soil samples. Soil samples were dried at 105 °C for approximately 10 h. Then, the samples were ground up and sieved. Soil samples were mixed with de-ionized water to achieve a moisture content of 28% and stored for use. The test temperatures of soil were controlled at 25, 35, 45, 55, 65 and 75 °C using a water bath.

Table 1. Compositions and pH value of soil samples from Zunyi, (wt%)

pH	Salt	SO ₄ ²⁻	Cl ⁻	NO ₃ ⁻	HCO ₃ ⁻	Ca ²⁺	Mg ²⁺	K ⁺	Na ⁺
4.9	0.0376	0.0097	0.0082	0.0018	0.036	0.0094	0.0011	0.0012	0.0015

2.3 Electrochemical tests

Electrochemical tests were conducted using a PARSTAT 2273 system. A three-electrode scheme was used: the working electrode was made of X80 steel, while graphite and Cu-CuSO₄ were employed as the auxiliary and reference electrodes, respectively. Electrochemical impedance spectroscopy (EIS) tests were performed at the open circuit potential (OCP). EIS spectra were recorded in a frequency range between 10⁴ and 0.005 Hz. The polarization curves were scanned by polarizing the samples ±150 mV versus OCP with a scanning rate of 0.166 mV/s. To examine the reproducibility, each test was repeated three times.

3. RESULTS AND DISCUSSION

3.1 Potentiodynamic polarization measurement

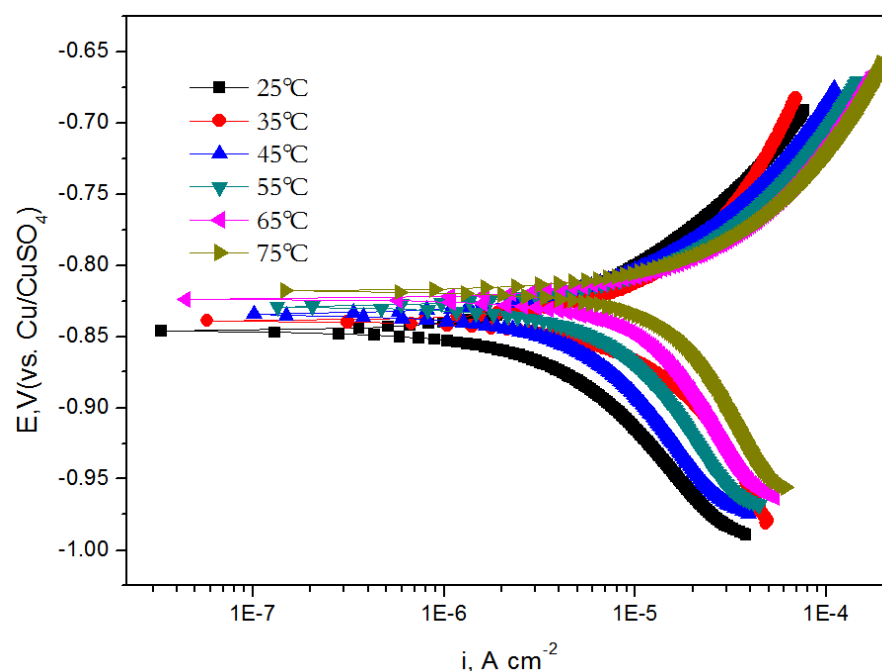


Figure 1. Potentiodynamic polarization curves of X80 steel after burying for 24 h at the temperature range 25 °C to 75 °C

Table 2. Fitted results for polarization curves of X80 steel after burying for 24 h at the temperature range 25 °C to 75 °C

Temperature ◻ °C	i _{corr} , μA·cm ⁻²	E _{corr} ◻ mV	β _c , mV/dec	β _a ◻ mV/dec
25	5.48	-846	199	127
35	11.31	-835	397	146
45	23.64	-829	419	175
55	46.49	-823	521	217
65	58.39	-818	545	233
75	107.20	-815	615	313

The polarization curves of X80 steel after burying for 24 h at the temperature range 25 °C to 75 °C are shown in Fig. 1. The shapes of the polarization curves are similar, suggesting the same corrosion process. The passivating regions are not observed in the anodic polarization curves at all temperatures, as shown in Fig. 1, which indicates that the steel corrosion is controlled by the activating reaction. Table 2 shows that the anodic and cathodic Tafel slopes increase with increasing temperature, and at the same temperature, the increasing rate of the β_c slope is much faster than that of the β_a slope. The above results show that the temperature influences not only the anodic reaction but also the cathodic reaction, and the effect of the temperature on the cathodic reaction is more severe.

Table 2 also shows that with increasing temperature from 25 to 75 °C, the i_{corr} value increases from 5.48 to 107.20 $\mu\text{A}/\text{cm}^2$. The increase in the corrosion current density indicates that the corrosion rate (CR) of X80 steel increases with increasing soil temperature because the corrosion rate has a positive relationship with the corrosion current density. The CR of X80 steel at 75 °C is 19 times higher than that at 25 °C. With increasing temperature, the diffusion rate of ferrous ions toward bulk soil increases, and the ferrous concentration on the soil/steel interface decreases, which lead to an increase in the dissolution rate of irons. At the same time, the diffusion rate of oxygen toward the interface also increases with increasing temperature, which enhances the cathodic reduction of the oxygen. The two reasons mentioned above both accelerate the corrosion of X80 steel in an acidic soil.

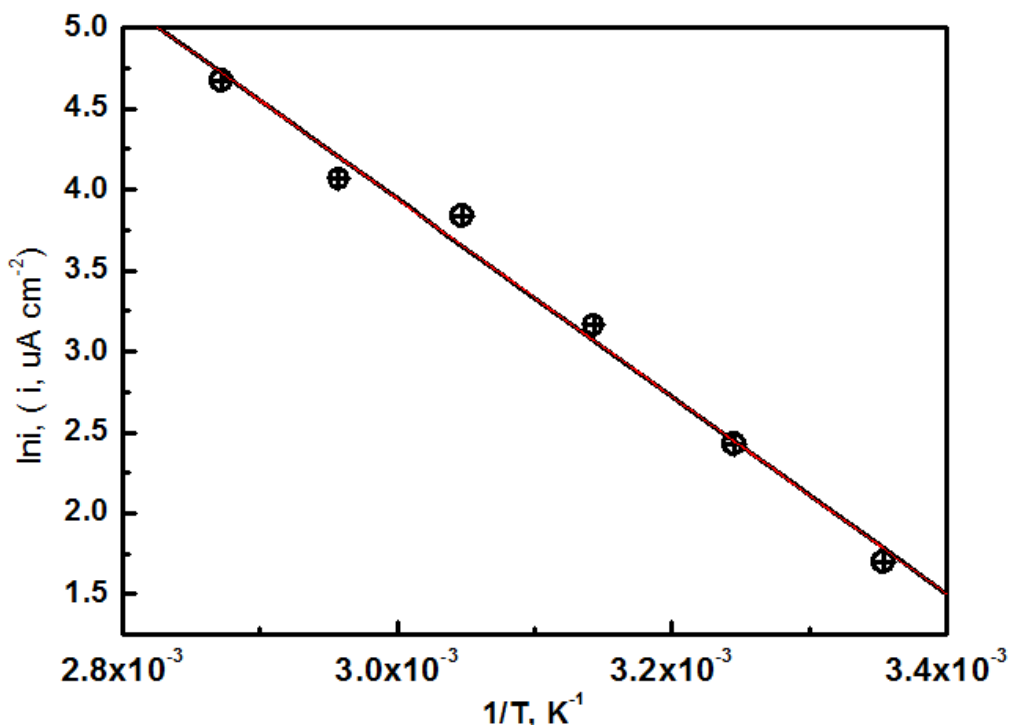


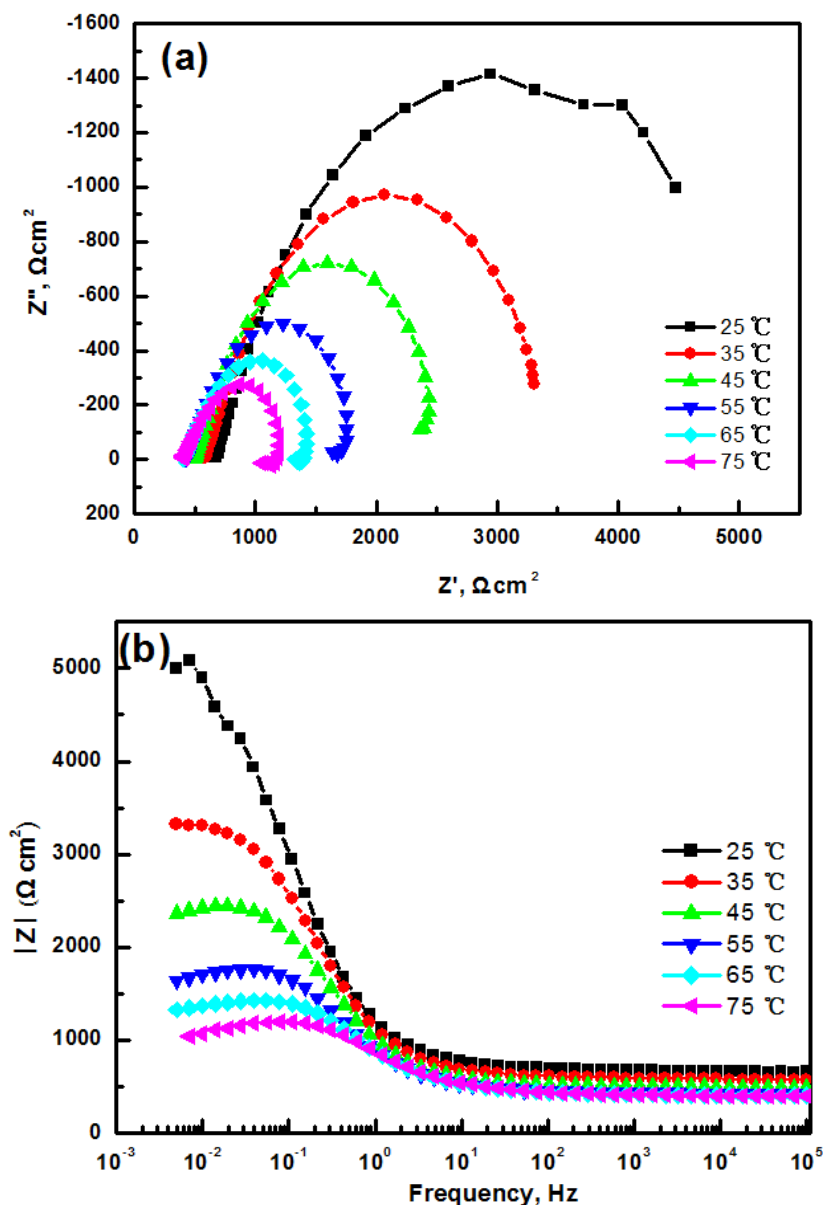
Figure 2. Arrhenius plot obtained from corrosion current density relationship with temperature

The activation energy of corrosion reaction can be determined from the Arrhenius formula [20, 21]:

$$\ln i_{corr} = -\frac{E_a}{R} \frac{1}{T} + \ln A \quad (1)$$

where E_a is the activation energy, i_{corr} the corrosion current density, A the pre-exponential constant, T the soil temperature in absolute and R the universal gas constant. Fig.2 illustrates the Arrhenius plot obtained from corrosion current density relationship with temperature. E_a was obtained from the slope of Arrhenius graph given in Fig.2 and was calculated to be $E_a = 50.7 \text{ kJ}\cdot\text{mol}^{-1}$ (Correlation coefficient $r^2=0.985$). As E_a of corrosion reaction was greater than $20 \text{ kJ}\cdot\text{mol}^{-1}$, the whole corrosion process was surface-reaction controlled [22].

3.2 Electrochemical impedance spectra measurement



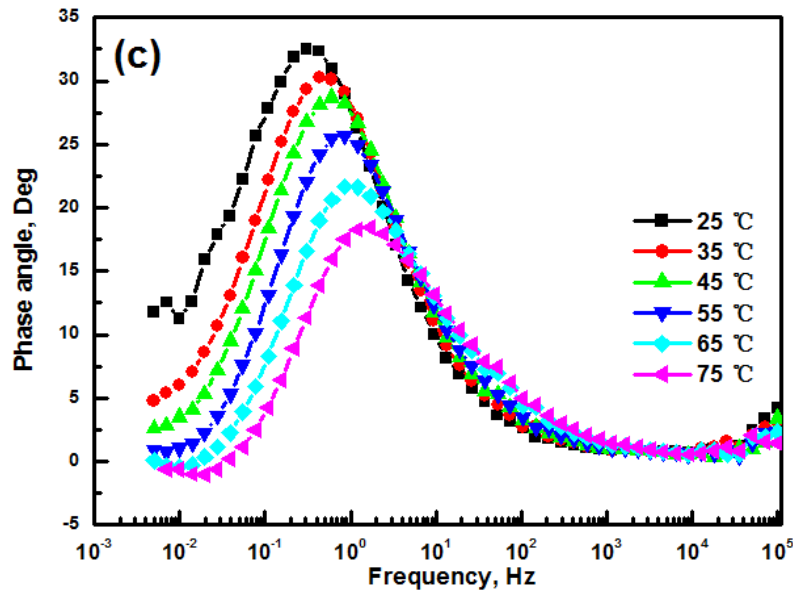


Figure 3. EIS of X80 steel after burying for 24 h at the temperature range 25 °C to 75 °C

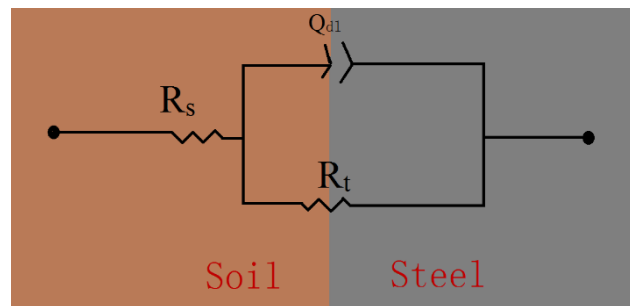


Figure 4. Equivalent circuit for the EIS

Table 3. Fitted results for EIS of X80 steel after burying for 24 h at the temperature range 25 °C to 75 °C

Temperature ◻ °C	R _s , Ω·cm ²	Y ₀ , S ⁿ ·Ω·cm ⁻²	n	R _t ◻ kΩ·cm ²
25	671.9	3.788×10 ⁻⁴	0.6741	4.923
35	587.4	3.478×10 ⁻⁴	0.7085	2.977
45	502.8	3.559×10 ⁻⁴	0.7241	2.093
55	436.2	3.671×10 ⁻⁴	0.7289	1.395
65	413.4	3.379×10 ⁻⁴	0.6951	1.057
75	409.3	2.876×10 ⁻⁴	0.6948	0.795

Fig. 3 shows the electrochemical impedance spectra (EIS) of X80 steel after burying for 24 h at the temperature range 25 °C to 75 °C. From the Nyquist diagram of Fig. 3a, it can be seen that the electrochemical impedance spectra of X80 steel have one time constant. The Nyquist plots are not standard semicircles, which can be attributed to the frequency dispersion [23-26]. The radius of the capacitive arc decreases gradually with increasing soil temperature.

The Bode diagrams in Fig. 3b present the changes in the impedance spectrum modulus $|Z|$. The magnitudes of the horizontal section modulus in the low frequency region reflect the change in the polarization resistance. It can be found that with increasing soil temperature, the modulus of the impedance spectrum in the low frequency region decreases, indicating that the reaction resistance of X80 steel decreases.

The Bode diagrams in Fig. 3c reflect the changes in the phase angle with frequency. It can be observed that the phase angle maximum decreases and the frequency corresponding to the maximum phase angle shifts to the higher frequency region with an increase in temperature. Within the temperature range studied, the EIS of X80 steel did not show the Warburg impedance characteristic being controlled by the diffusion process, revealing that the oxygen diffusion from soil to the X80 steel surface and the corrosion products are not enough to hinder the mass transfer process of the corrosion reaction and becomes the control step of corrosion.

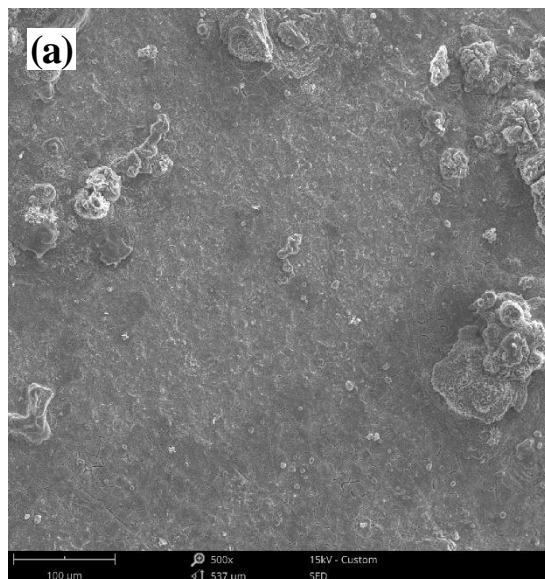
The equivalent circuit of the EIS is given in Fig. 4. Impedance for the circuit of Fig. 4 can be expressed by the following Eq. (2).

$$Z = R_s + \frac{R_t}{R_t Y_0 (\omega j)^n} \quad (2)$$

where R_s is a representative of soil resistance, R_t refers to the charge transfer resistance of X80 steel and Q_{dl} represented constant phase element (CPE) associated with the dispersion of a capacitance [17, 27]. The impedance of Q_{dl} is written as $Z_Q = Y_0^{-1} (j\omega)^{-n}$, where ω is angular frequency, n and Y_0 are the CPE parameters [28-30].

The plots are fitted using ZSimpWin software, and the results are shown in Table 3. From Table 3, we can observe that the R_t values decrease with increasing soil temperature. R_t is a physical quantity that is inversely proportional to the CR; the lower the R_t , the higher the CR. With the increase of soil temperature, the R_t values of X80 steel decreased, implying that soil with a high temperature is linked to a high CR. The results coincide well with those of the polarizing curve investigations.

3.3 Surface analysis



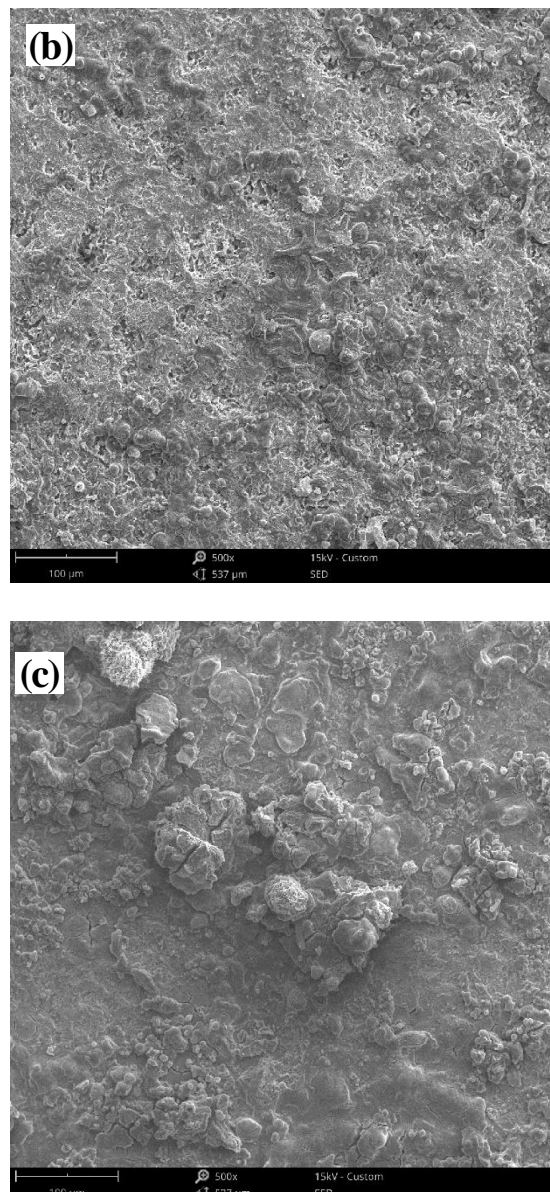
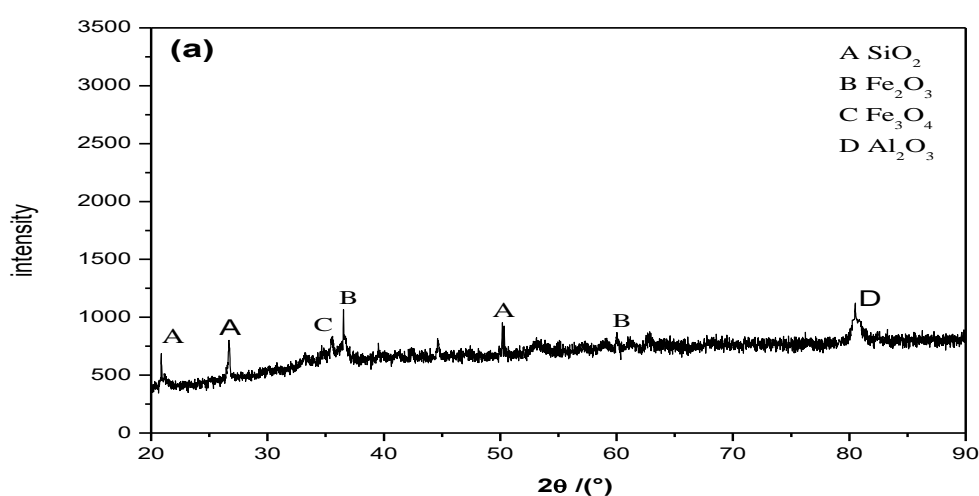


Figure 5. SEM images of X80 steel after burying for 240 h at different temperatures : (a) 25 °C, (b) 55 °C, (c) 75 °C



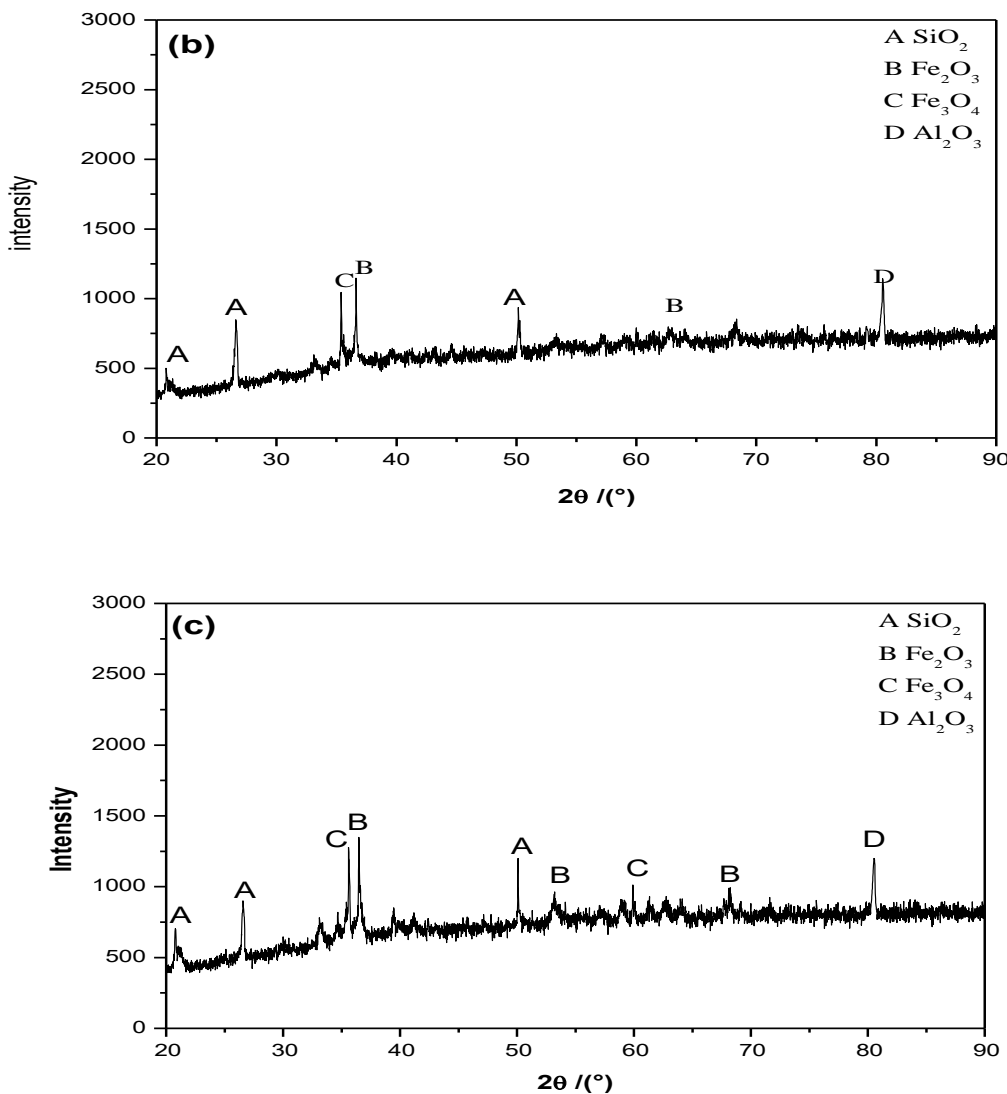


Figure 6. XRD spectra of the corrosion products of X80 steel after burying for 240 h at different temperatures: (a) 25 °C, (b) 55 °C, (c) 75 °C

Fig. 5 presents SEM images of X80 steel in the soil at different temperatures after it was buried for 240 h. It is evident that the surface of X80 steel at 25 °C displays a homogeneously corroded area, as shown in Fig. 5a. With increasing temperature, the corrosion products become loose and heterogeneous on the surface of the steel. The surface roughness of X80 steel increases with increasing soil temperature. The variation in the corrosion product layer on the steel surface further enhances the corrosion of X80 steel, which also verifies the results of the electrochemical measurements. Wang et al. [31] and Suganya et al. [32] have also reported that the corrosion rates of steel increase with increasing surface roughness. To further investigate the compositions of the corrosion products, the products were analyzed by X-ray diffraction (XRD), as shown in Fig. 6. Clearly, the corrosion products consisted of Fe_2O_3 , Fe_3O_4 and some soil components such as SiO_2 and Al_2O_3 .

4. CONCLUSIONS

(1) The i_{corr} of X80 steel in an acidic soil increased from 5.48 to 107.20 $\mu\text{A}/\text{cm}^2$ with increasing soil temperature from 25 °C to 75 °C, and the CR at 75 °C was 19 times higher than that at 25 °C.

(2) The R_t decreased with increasing soil temperature, and the control step for corrosion was the activation of the polarization process.

(3) The compositions of corrosion products consisted of Fe_2O_3 , Fe_3O_4 and some soil components such as SiO_2 and Al_2O_3 .

(4) The kinetics of the corrosion process complied with Arrhenius law, and the E_a determined using the Arrhenius plot was 50.7 $\text{kJ}\cdot\text{mol}^{-1}$, indicating the corrosion process was under surface-reaction control.

ACKNOWLEDGEMENTS

This work was supported by the Natural Science Foundation of China (No. 51561033), the Special Key Laboratory of Electrochemistry for Materials of Guizhou Province (No.QJHXYZ[2018]004), and the Guizhou Provincial Science and Technology Foundation (No. LH[2017]7067).

References

1. S. Handley-Sidhu, N. D. Bryan, P. J. Worsfold, D. J. Vaughan and F. R. Livens, *Chemosphere*, 77 (2009)1434.
2. I. I. Cole and D. Marney, *Corr. Sci.*, 56 (2012)5.
3. Z.Y. Liu, Q. Li, Z.Y. Cui, W. Wu, Z. Li, C.W. Du and X.G. Li, *Constr. Build. Mater.*, 148 (2017)131.
4. J. Xu, K.X. Wang, C. Sun, F.H Wang, X.M. Li, J.X. Yang and C.K Yu, *Corros. Sci.*, 53 (2011)1554.
5. T.Q. Wu, J. Xu, M. C. Yan, C. Sun, C. Yu and W. Ke, *Corros. Sci.*, 83 (2014)38.
6. Y.H. Wu, T.M. Liu, S.X. Luo and C. Sun, *Materialwiss. Werkstofftech.*, 41 (2010)142.
7. C.M. Yan, C. Sun, J. Dong, J. Xu and W. Ke, *Corros. Sci.*, 97 (2015)62.
8. Y. H. Wu, T. M. Liu, C. Sun, J. Xu and C. K. Yu, *Corr. Eng. Sci. Techn.*, 45 (2010)136.
9. X. H. Nie, X. G. Li, C. W. Du and Y. F. Cheng, *J. Appl. Electrochem.*, 39 (2009)277.
10. L. S. Mcneill and M. Edwards, *Environ. Monit. Assess.*, 77 (2002) 229.
11. P. Kritzer and J. Supercrit, *Fluids*, 29 (2004)1.
12. F. Xie, D. Wang, M. Wu, C.X. Yu , D.X. Sun, X. Yang and C.H. Xu, *Metal. Mater.Trans. A*, 49 (2018)1372.
13. I. S. Cole and D. Marney, *Corros. Sci.* 56 (2012)5.
14. W. Guo, H. Dong, M. Lu and X. Zhao, *Int. J. Pres. Ves. Pip.*, 79 (2002)403.
15. P. Liang, Y.Guo, H.Qin, Y.H.Shi, F. Li, L.Jin and Z. Fang, *Int. J. Electrochem Sci.*, 14(2019)6247.
16. Y. H. Wu, S.X. Luo and H. Gou, *Sur. Tech.*, 42(2012)12.
17. Y.H. Wu, S.X. Luo and H. Gou, *Materialwiss. Werkstofftech.*, 43 (2012)1074.
18. L.M. Quej-Ake and A. Contreras, *Anti-Corros. Method. M.*, 65 (2018)97.
19. Nguyen Dang, L. Lanarde, M. Jeannin, R. Sabot and Ph. Refait, *Electrochim. Acta*, 176 (2015)1410.
20. Rashid, Khalid, Khadom and Anees, *Anti-Corros. Method. M.*, 65 (2018)506.
21. T. Debenest, F. Gagné , A. N. Petit, C. André, M. Kohli and C. Blaise, *Comp. Biochem. Physiol., Part C: Toxicol. Pharmacol.*, 152 (2010)407.
22. S.K. Shukla and M.A. Quraishi, *J. Appl. Electrochem.*, 39 (2009) 1517.
23. F. Bentiss, M. Lagrenée, M. Traisnel, B. Mernari and H. El Attari., *J. Appl. Electrochem.*, 29

- (1999)1073.
- 24. Z. Stoynov, B. Grafov, B. Savova-Stoynova and V. Elkin., *Electrochemical Impedance*, Nauka, Moscow, 1991.
 - 25. F. Bentiss, M. Traisnel and M. Lagrenée., *Corros. Sci.*, 42 (2000)127.
 - 26. Motsie M., Olasunkanmi Lukman, Adekunle Abolanle, Yesudass Sasikumar, Kabanda Mwadham and Ebenso Eno., *Materials*, 8 (2015)3607.
 - 27. X. X. Sheng, Y. P. Ting and S. O. Pehkonen, *Corros. Sci.*, 49 (2007)2159.
 - 28. K. Mallaiya, R. Subramaniam, S.S. Srikandan, S. Gowri, N. Rajasekaran and A. Selvaraj, *Electrochim. Acta*, 56 (2011) 3857.
 - 29. C. H. Hsu and F. Mansfeld, *Corrosion*, 57 (2001)747.
 - 30. B. Perez-Navarrete, C. O. Olivares-Xometl and N. V. Likhanova, *J. Appl. Electrochem.*, 40 (2010)1605.
 - 31. H.B. Wang, Y. Li, G.X. Cheng, W. Wu, Y.B. Zhang, X.Y. Li, *Int. J. Electrochem Sci.*, 13(2018)5268.
 - 32. S. Suganya and R. Jeyalakshmi, *J. Mater. Eng. Perform.*, 28 (2019)863.

© 2020 The Authors. Published by ESG (www.electrochemsci.org). This article is an open access article distributed under the terms and conditions of the Creative Commons Attribution license (<http://creativecommons.org/licenses/by/4.0/>).